ULTRASONIC WAVE PROPAGATION AND ATTENUATION IN WET BONE

Roderic Lakes, Hyo Sub Yoon and J. Lawrence Katz

Received February 1985, revised November 1985

ABSTRACT

The propagation of ultrasonic longitudinal waves in bovine plexiform and human Haversian bone has been studied over the range 0.5–16 MHz. In wet bone little velocity dispersion was observed, in contrast to the results of earlier studies on dry bone. Large values of attenuation were observed.

Keywords: Bone; ultrasonics

INTRODUCTION

Ultrasonic studies of bone and other calcified tissues are motivated principally by two considerations: achieving a greater understanding of the role of microstructure in determining the mechanical properties of the tissue, and developing clinical diagnostic tools for the assessment of disease states. Among basic studies are the experiments by Yoon and Katz[1,2] and Lang[3] in which the texture symmetry and the full set of anisotropic elastic constants were determined. Human Haversian bone behaves as a quasi-hexagonal or axisymmetric material with five independent elastic constants[2,3]. Bovine plexiform bone behaves as an orthotropic material with nine independent elastic constants[4]. Recently it has been suggested that human bone is also orthotropic in its mechanical properties[5], albeit the deviations from hexagonal symmetry are small.

In the clinical domain, efforts have been made to use ultrasound to diagnose a variety of skeletal disorders. For example, changes in the waveforms of propagated ultrasonic waves have been related to the degree of healing of fractures by Brown and Mayor[6]. A device based on detection of the magnetic field produced by ultrasonic waves in bone via the piezoelectric effect was developed by Lakes and Saha[7] to avoid artifacts due to soft tissue properties. Acoustic emission methods were used by Yoon *et al*.[8] to explore effects associated with surgical defects and microdamage in bone under load.

It is the purpose of this investigation to examine the dispersion and attenuation of ultrasonic waves in bone to provide an insight into structure-related micromechanical processes and characteristics of bone tissue, and to understand how simulated acoustic emission signals are propagated in bone in the clinical application of acoustic emission techniques.

Department of Biomedical Engineering, Rensselaer Polytechic Institute, Troy, NY 12181, USA
Reprints from Professor R. Lakes, Department of Biomedical Engineering, The University of Iowa, Iowa City, IA 52242, USA

EXPERIMENTAL METHODS

Specimen preparation

Fresh-frozen femoral compact bone from cows, and femoral compact bone from a human cadaver were used for this investigation. Bovine specimen B_1 was taken from the lateral aspect of the midshaft of a femur. Human bone specimens were cut from the lateral aspect of the femoral midshaft from a female subject aged 56 years. Specimens H_{1a}, H_{1b}, H_{2a}, H_{2b} were from adjacent areas of this bone. Specimens were cut while wet, into rectangular parallelepipeds with an Isomet low-speed diamond saw (Buehler Ltd., Lake Bluff, IL). The specimen axes were aligned with the microstructural symmetry axes of the bone tissue. Specimens were frozen when not under study and were kept wet in Ringer's solution with penicillin and streptomycin between experiments. Specimen dimensions were as shown in *Table 1*.

The surface of each specimen was ground and polished using the usual metallographic techniques, all were mounted on an alignment device with double sided adhesive tape and ground with graded abrasives on a strip grinder (Handimet, Buehler Ltd.). The structural orientation was then checked by reflected light microscopy.

Table 1 Dimensions of samples

	Length (mm)	Circumferential length (mm)	Radial length (mm)
Bovine B_1	15.82	9.45	6.65
Human H_{1a}	10.41	5.64	3.21
Human H_{1b}	5.86	5.64	3.21
Human H_{2a}	10.84	4.06	1.78
Human H_{2b}	10.84	2.21	1.78

0141-5425/86/020143-06 $3.00

Ultrasonic measurements

In this study, electrical pulses were generated by a Matec (Warwick, RI) 6600 pulser/receiver, or by an Arenberg (Jamaica Plain, MA) pulser. The electrical pulses were fed into a broadband piezoelectric transducer (Panametrics, Waltham, MA). Transducers of resonant frequency 1.0, 2.25, 5.0 and 10.0 MHz were used to generate longitudinal waves in the specimen and experiments were conducted at room temperature (23.5 ± 0.5°C), with water as a couplant.

Three kinds of ultrasonic velocity measurements were made. First, wave packets containing from seven to ten oscillations were generated and the transmission delay of the peak of the pulse envelope through the specimen was measured on an oscilloscope (Tektronix type 465 with digital time delay indicator). The group velocity was then calculated by dividing the specimen thickness by the time delay. Second, long wave packets containing many oscillations were used and time delay measured from the leading edge of the waveform. The first oscillation in the leading edge which exceeded one third the maximum amplitude, was identified and the zero crossing following that peak used to determine the signal time delay. The signal velocity was then calculated from the delay. Third, phase velocities were determined using a pulse echo overlap method. In this method, pairs of echoes are compared by driving the horizontal input of an oscilloscope at a frequency equal to the reciprocal of the travel time between the echoes[9–11]. The method outlined by Papadakis[10] was applied to achieve a proper cycle for cycle match between the two echoes, to obtain the phase delay, and hence also the phase velocity. In this investigation a buffer rod of polymethyl methacrylate (PMMA) was used, as shown in *Figure 1a*. The buffer served to delay the echoes so they would not be masked by ringing from the drive pulse. The buffer rod diameter was sufficiently large (50 mm) in relation to its thickness (25 mm) to ensure that echoes from its cylindrical boundary did not obtrude into the received signal.

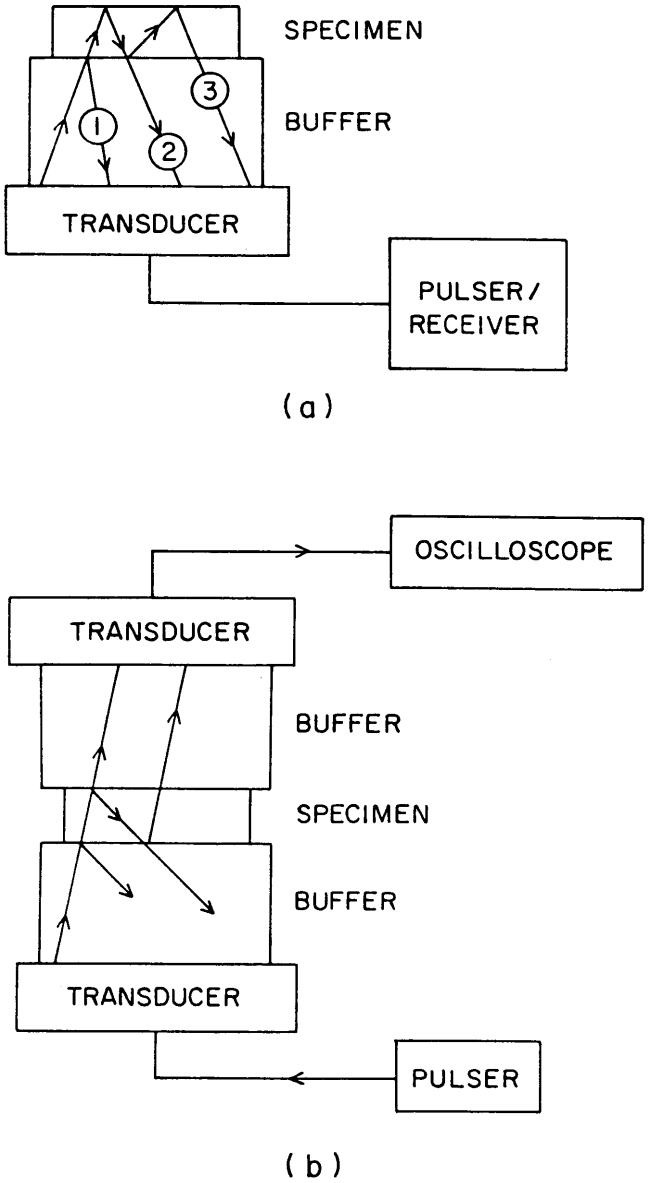

Figure 1 Configuration of transducers for ultrasonic measurements. a, Single transducer arrangement for pulse echo measurements. b, Two transducer system for echo and transmission measurements. Paths of the various reflected waves are indicated schematically by arrows

The pulse echo overlap method was also used to collect measurements of attenuation in bone. Again the buffer configuration shown in *Figure 1a* was used. By contrast, in the original versions of this method[9,10] a quartz transducer was bonded directly to the specimen. Such an approach would not be satisfactory for experiments upon bone for the following reasons. Bone specimens can only be obtained in relatively small sizes if measurements in the radial and circumferential directions are to be made; as a consequence, short wave packets with negligible ringing must be used. Broadband transducers with large coupling coefficients and significant internal damping were used in this study. In contrast to the bonded quartz transducers described by Papadakis[10], our transducers, by virtue of the absorption of acoustic energy, would introduce unacceptable attenuation errors if bonded to the specimen. To minimize these problems a buffer rod was used[11].

Attenuation was calculated as follows. Following Papadakis[11] the attenuation α is given by

$$\alpha = [\ln(-R/(A_3/A_2))]/2t$$

in which t is the specimen thickness, R is the reflection coefficient for the buffer-specimen interface, and A_1, A_2 and A_3 are the (signed) amplitudes of subsequent echoes. The first echo amplitude A_1 can be used to calculate R, but does not explictly appear in the equation for α. Since the specimen was smaller than the end of the buffer rod, the first echo contained reflections from a specimen–buffer and an air–buffer interface. Therefore, the method of Papadakis[11] for calculating R from the echo amplitudes could not

be used. Instead, R was calculated from the acoustic impedances of the specimen Z_S and buffer, Z_B:

$$R = \frac{Z_B - Z_S}{Z_B + Z_S}$$

The acoustic impedances, given by $Z = \rho V$, were calculated from the density ρ and wave velocity V of each material.

Errors in the calculated attenuation depend on errors in the measured echo amplitudes and reflection coefficient. Errors are minimized when the reflection coefficient is between 0.4 and 0.6, as was the case in this study. Estimated errors in the results are 10–15% in the attenuations and 1% in the velocities.

It was not possible to measure attenuations over the full frequency range 1–16 MHz using the pulse echo method, due to the large values of attenuation observed at the higher frequencies. Specifically, it was necessary in this method to observe two subsequent echoes to determine the attenuation. The second echo, after traversing a distance equal to four times the specimen thickness, became excessively attenuated at frequencies above 6 MHz. The transmission configuration of *Figure 1b* was therefore used to infer attenuations at higher frequencies; in this configuration the wave packet need only traverse the specimen once. The attenuation at a frequency ν_1 is given by

$$\alpha(\nu_1) = \alpha(\nu_0) + \frac{1}{t} \ln [T(\nu_0)/T(\nu_1)]$$

in which t is the specimen thickness, $T(\nu_0)$ is the transmission coefficient of the specimen at frequency ν_0 and $T(\nu_1)$ is the transmission coefficient at frequency ν_1. $\alpha(\nu_0)$ is the absolute attenuation at frequency ν_0 (here 5 MHz) as determined by the pulse echo method. The acoustic impedance mismatch between specimen and buffer does not appear in this expression since it was assumed to be independent of frequency, an assumption considered justified in view of the smallness of the velocity dispersion in bone and PMMA.

The loss tangent was calculated from the attenuation α to facilitate comparison with the results of viscoelastic measurements obtained elsewhere under quasistatic sinusoidal loading. The loss tangent $\tan \delta$ is given by[12]

$$\tan \frac{\delta}{2} = \frac{\alpha v}{2\pi\nu}$$

in which v is the wave velocity and ν is the frequency.

RESULTS

The group velocity, phase velocity, signal velocity and loss tangent of longitudinal waves in bovine bone are plotted in *Figure 2*. The signal velocity and loss tangent for human bone are shown in *Figure 3* and the attenuation for both bovine and human bone in *Figure 4*.

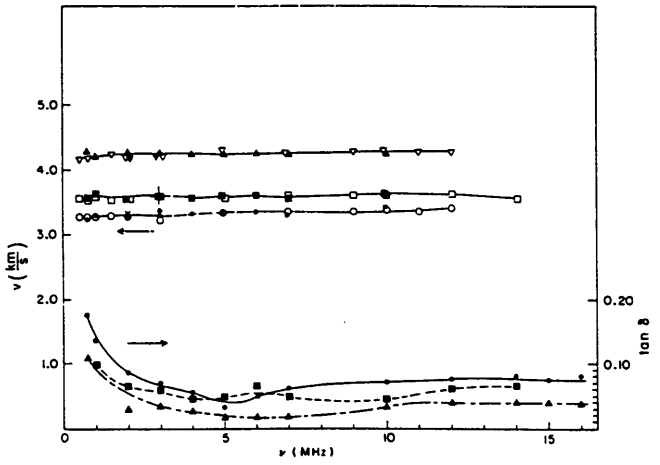

Figure 2 Velocity and loss tangent in bovine bone. Group velocity; loss tangent: ▲, longitudinal direction; ■, circumferential direction; ●, radial direction. Signal velocity: ▽, longitudinal direction; □, circumferential direction; ○, radial direction. Phase velocity: ▼, longitudinal direction; +, circumferential direction; ×, radial direction

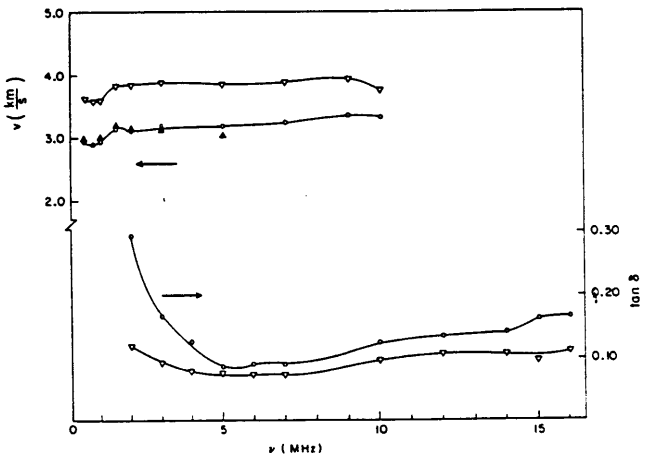

Figure 3 Signal velocity and loss tangent in human bone. ▽, longitudinal direction; ▲, circumferential direction; ○, radial direction

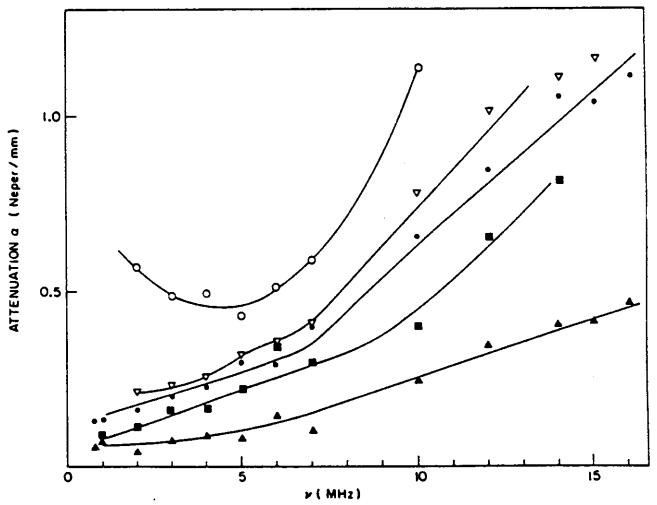

Figure 4 Attenuation in nepers per mm. Bovine bone, solid symbols as in *Figure 2*. Human bone, open symbols

In wet bovine bone, there was essentially no dispersion of velocity. In a nondispersive medium, the phase, group and signal velocities should be identical and as will be seen from *Figure 2* these velocities do indeed coincide. Human bone exhibited some dispersion at the lower frequencies (*Figure 3*). Our results contrast with dispersion measurements performed on dry bone, in which for longitudinal waves propagating along the bone axis, the signal velocity dispersion was 2.9% and perpendicular to the bone axis it was 10.7% over the frequency range 2–10 MHz[13]. Sound velocity in dry bone was found to depend linearly on frequency[13].

In the course of this study, a new kind of longitudinal wave was observed, which travelled more slowly than was expected. This wave was not foreseen in the design of the experiments; the interested reader is referred to a previously published report[14].

DISCUSSION

In a material of biological origin, variations in physical properties may be expected to occur as a result of differences in structure and composition. It is therefore not surprising that in a larger group of specimens of wet bone, dispersion has recently been observed in some specimens[4]. Nevertheless, these dispersion values are considerably less than those from dry bone. Our results and those of Reference 4 support the conclusion that wet bone is less dispersive than dry bone. In the human bone examined in this study, the dispersion exhibited at the lower frequencies is attributed to a geometrical cause: the transition from extensional to longitudinal wave motion. The corresponding transition in the bovine bone would be below the lowest frequency used here, due to the larger size of that specimen.

The attenuation results obtained in this study may be compared with those of other investigators. Few studies of wave attenuation in compact bone have been reported. Adler and Cook[15] measured the attenuation of longitudinal waves in wet canine (Haversian) tibial bone at 22°C: 13 dB/cm at 3 MHz and 19 dB/cm at 5 MHz, values which are equivalent to 0.14 nepers/mm and 0.22 nepers/mm, respectively. They lie between the values obtained by us for human bone (0.23 nepers/mm at 5 MHz) and bovine bone (0.067 nepers/mm) in the longitudinal direction. Attenuation in bone significantly exceeds that in polymethyl methacrylate[16] (PMMA), 0.018 nepers/mm at 1 MHz and 21.1°C, but it is comparable with values obtained in composites, e.g., 0.26 nepers/mm at 2 MHz in a random particulate composite[17], and 0.14 nepers/mm at 2.75 MHz in a fibrous composite[18].

Expressed in terms of the loss tangent, our attenuation results may be compared with viscoelastic measurements on bone at lower frequencies. Specifically, the loss tangent of human and bovine bone is approximately 0.01 in torsion between 1 and 100 Hz[19] and is 0.01 and 0.02 in bending between 100 Hz and 1 kHz[20]. The loss tangents determined from our measurements at ultrasonic frequencies are by contrast significantly larger, by a factor of up to thirty. It may therefore be of interest to examine some of the loss mechanisms which can act at ultrasonic frequencies.

Attenuation mechanisms in bone may be considered in relation to its microstructure, however definitive identification of mechanisms is rendered difficult by the complexity of the bony microstructure. Specifically, bone may be regarded as a composite with particulate, porous and fibrous structural elements at different levels of scale; the nature and typical size of these structural elements are shown in *Table 2*. The microstructure of human compact bone is shown in *Figure 5* and the microstructure of bovine plexiform bone in Reference 14. In the sequel, we discuss hypothetical wave attenuation mechanisms in bone in the context of results for simpler materials.

Scattering of waves from inhomogeneities has been identified as an attenuation mechanism in various synthetic composites[17,21]. In composites with a regular periodic structure, a sharp maximum in the attenuation is expected when the ultrasonic wavelength equals twice the size of the unit cell in the propagation direction[18]. This condition corresponds to a cut-off frequency at which the wavespeed drops to zero. Such frequencies, calculated for bone, are displayed in *Table 2*. Experimental evidence for the above mentioned phenomena has been found in composites with regular periodic microstructures[18], but not in those with random microstructures[17]. We found no evidence of a cut-off frequency; its absence in bone may be attributed to aperiodicity in the microstructure of bone, and/or stiffening of the cement substance between osteons or laminar by virtue of its viscoelasticity. The cement substance is thought to be highly compliant or even viscous[22]

Table 2 Structural elements of bone

Structural feature	Role in composite structure	Size (μm)	Frequency (MHz) for size = $\lambda/2$
Osteons (human) Laminae (bovine)	Fibre lamina	250	8
Haversian canals	Pore or fluid filled channel	50–150	40–13
Osteocyte lacunae	Pore	10–25	80–200
Lamella	Lamina	5	400
Collagen fibre	Fibre	1–2	2000–1000
Apatite crystals	Particulate inclusion	0.005–0.05	400×10^3–40×10^3

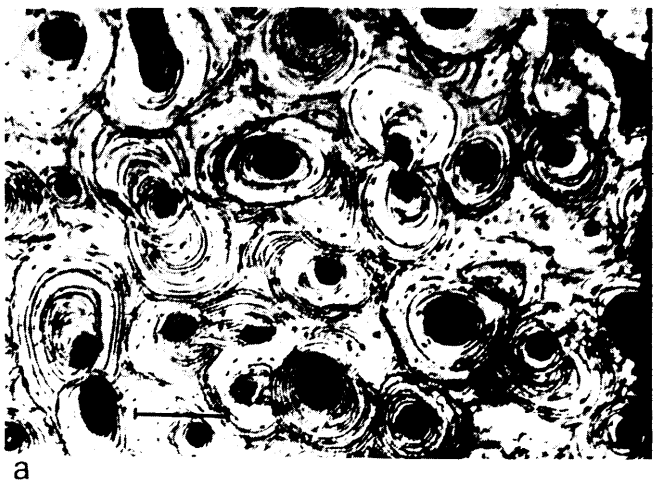

a

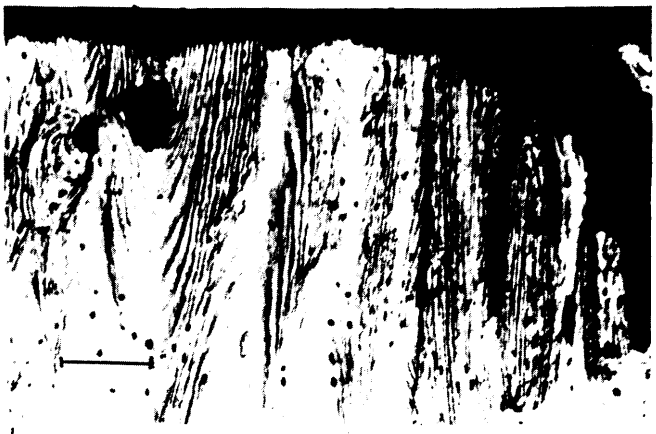

b

Figure 5 Microstructure of human Haversian bone H_1. Reflected light micrograph. a, Cut surface perpendicular to longitudinal direction. b, Radial direction. Scale mark, 0.20 mm

under quasistatic loading, but there is evidence that it is nearly as stiff as the osteon itself at ultrasonic frequencies[23]. If that were the case, effects due to the fibrous or laminar architecture of bone might be weak or absent at ultrasonic frequencies.

An additional wave attenuation mechanism may be encountered in materials with interconnected, fluid-filled pores. The dynamics of the fluid–solid interaction are predicted to result in attenuation of acoustic waves[24,25], an attenuation which depends upon the geometry and volume fraction of pores; it can become large in some situations. In the case of wet compact bone, the interconnected, fluid-filled pores are of a much more complex geometry than assumed in the theory. A quantitative comparison, consequently, is not easily achieved.

Relationship to acoustic emission studies

The inverse of the attenuation, α, represents a decay depth: a distance over which the wave amplitude decays to 1/e of its original value. Referring to *Figure 4*, we observe that over much of the frequency range, longitudinal acoustic waves cannot penetrate more than a millimeter or two without becoming severely attenuated. The attenuation is particularly large in the case of human bone in the radial direction. Consequently, acoustic emission methods based on signals at or above 0.5 MHz, for detecting microdamage in bone are sensitive only to events occurring near the bone surface. Although the frequency range for acoustic emission may be from zero to 100 MHz, studies on bone have utilized a band from 100 to 300 kHz[26]. In this latter range a signal would propagate as a kind of Lamb mode of wavelength greater than the bone's cortical thickness. The application to such a situation of our attenuation results for bulk waves may be less than straightforward.

CONCLUSIONS

The following conclusions are drawn from the results of this study.

Ultrasonic waves in wet human and bovine bone exhibit little dispersion of velocity. Consequently the phase, group and signal velocities were virtually identical. The use of wet bone permits different measurement techniques to be employed to obtain comparable values for the ultrasonic velocity.

Large values of ultrasonic attenuation in bone were observed. Attenuation of ultrasonic waves in wet human bone in the radial direction was sufficiently large to limit the penetration depth to 2 mm or less. Techniques based on transmission of high-frequency ultrasonic waves through bone are therefore unlikely to be of use clinically.

No evidence of a cut-off frequency was found. Microstructural resonance at the osteon level, if it occurs at all, does not manifest itself in ultrasonic transmission measurements.

ACKNOWLEDGEMENTS

This research was supported by the U.S. Department of Education through NIHR Grant No. G008200028. We thank Dr Alain Meunier for providing specimens and for many illuminating discussions.

REFERENCES

1 Yoon, H.S. and Katz, J.L. 'Ultrasonic wave propagation in human cortical bone I, theoretical considerations for hexagonal symmetry. *J. Biomech.*, 1976, **9**, 407
2 Yoon, H.S. and Katz, J.L. Ultrasonic wave propagation in human cortical bone II, measurements of elastic properties and microhardness, *J. Biomech.*, 1976, **9**, 459
3 Lang, S.B. Ultrasonic method for measuring elastic coefficients of bone and results on fresh and dried bovine bones, *IEEE Trans. Biomed. Eng.*, 1970, **17**, 101
4 Maharidge, R. Meunier, A. Yoon, H.S. and Katz, J.L. in preparation
5 Van Buskirk, W.C. and Ashman, R.B. The elastic moduli of bone. In: *Mechanical Properties of Bone,* (Ed. S.C. Cowin) ASME, New York, 1981, AMD Vol. 45, 131–143

6 Brown, S.A. and Mayor, M.B. Ultrasonic assessment of early callus formation, *Biomed. Eng.*, 1976, **11**, 124

7 Lakes, R.S. and Saha, S. A non-contacting electromagnetic device for the determination of *in vivo* properties of bone. *Med. Instru.*, 1978, **12**, 106

8 Yoon, H.S. Caraco, B. Kaur, H. and Katz, J.L. Clinical application of acoustic emission techniques to bone abnormalities. In: *1980 Ultrasonics Symposium Proceedings* (Ed. B.R. McAvoy) IEEE, New York, 1981, 1067–1072

9 May, J.E. *IRE Nat. Conv. Rec.*, 1958, **6**, 134

10 Papadakis, E. Ultrasonic phase velocity by the pulse echo overlap method incorporating diffraction phase corrections. *J. Acoust. Soc. Am.*, 1967, **42**, 1045

11. Papadakis, E. Ultrasonic velocity and attenuation: measurement methods with scientific and industrial applications. In: *Physical Acoustics*, (Eds W.P. Mason and R.N. Thurston) Academic Press, New York, 1976, Vol. XII, 277–374

12 Norris, D.M. Propagation of a stress pulse in a viscoelastic solid. *Experim. Mech.*, 1967, **7**, 297

13 Yoon, H.S. and Katz, J.L. Dispersion of the ultrasonic velocities in human cortical bone. In: *1976 Ultrasonics Symposium Proceedings* (Ed. J. de Klerk and B.R. McAvoy) IEEE, New York, 1976, 48–50

14 Lakes, R.S. Yoon, H.S. and Katz. J.L. Slow compressional wave propagation in wet human and bovine cortical bone. *Science* 1983, **220**, 513

15 Adler, L. and Cook, K.V. Ultrasonic parameters of freshly frozen dog tibia. *J. Acous. Soc. Am.*, 1975, **58**, 1107

16 Pearson, J.M. *A Theory of Waves*, Allyn and Bacon, Boston, 1966, 88–93

17 Kinra, V.K. Petraitis, M.S. and Datta, S.K. Ultrasonic wave propagation in a random particulate composite. *Int. J. Solids, Structures* 1980, **16**, 301

18 Sutherland, H.J. and Lingle, R. Geometric dispersion of acoustic waves by a fibrous composite. *J. Comp. Mat.*, 1972, **6**, 490

19 Lakes, R.S. Katz, J.L. and Sternstein. S.S. Viscoelastic properties of wet cortical bone: Part I, torsional and biaxial studies. *J. Biomechanics*, 1979, **12**, 657

20 Johnson, M. Rensselaer Polytechnic Institute, private communication (1982)

21 Papadakis, E.P. Ultrasonic attenuation caused by scattering in polycrystalline media. In: *Physical Acoustics* (Eds W.P. Mason and D. Thurston), Academic Press, New York, 1968, Vol. IV, 269–328

22 Lakes, R.S. and Saha. S. Cement line motion in bone. *Science*, 1979, **204**, 501

23 Katz, J.L. Anisotropy of Young's modulus of bone. *Nature*, 1980, **283**, 106

24 Biot, M.A. Theory of propagation of elastic waves in a fluid-saturated porous solid, Part I: low frequency range. *J. Acous. Soc. Am.*, 1956, **28**, 168

25 Biot, M.A. Theory of propagation of elastic waves in a fluid-saturated porous solid, Part II: higher frequency range. *J. Acous. Soc. Am.*, 1956, **28**, 179

26 Thomas, R.A. Yoon H.S. and Katz. J.L. Acoustic emission from fresh bovine femora. *Proc. IEEE 1977 Ultrasonics Symp.* 237–241